ACCOUNTS
of chemical research

Optical Two-Dimensional Fourier Transform Spectroscopy of Semiconductor Quantum Wells

STEVEN T. CUNDIFF,*,† TIANHAO ZHANG,‡,§
ALAN D. BRISTOW,† DENIS KARAISKAJ,† AND XINGCAN DAI†

†JILA, National Institute of Standards and Technology and University of Colorado, Boulder, Colorado 80309-0440, ‡Department of Physics, University of Colorado, Boulder, Colorado 80309-0390

RECEIVED ON FEBRUARY 25, 2009

Downloaded by RENMIN UNIV OF CHINA on October 2, 2009 | http://pubs.acs.org
Publication Date (Web): June 25, 2009 | doi: 10.1021/ar9000636

CONSPECTUS

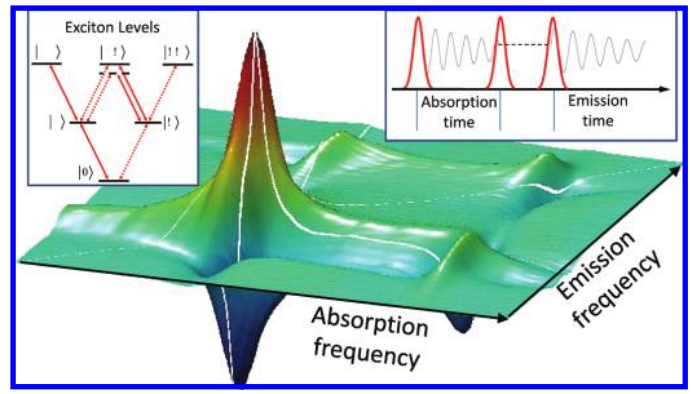

Coherent light−matter interactions of direct-gap semiconductor nanostructures provide a great test system for fundamental research into quantum electronics and many-body physics. The understanding gained from studying these interactions can facilitate the design of optoelectronic devices. Recently, we have used optical two-dimensional Fourier-transform spectroscopy to explore coherent light−matter interactions in semiconductor quantum wells. Using three laser pulses to generate a four-wave-mixing signal, we acquire spectra by tracking the phase of the signal with respect to two time axes and then Fourier transforming them. In this Account, we show several two-dimensional projections and demonstrate techniques to isolate different contributions to the coherent response of semiconductors.

The low-temperature spectrum of semiconductor quantum wells is dominated by excitons, which are electron−hole pairs bound through Coulombic interactions. Excitons are sensitive to their electronic and structural environment, which influences their optical resonance energies and line widths. In near perfect quantum wells, a small fluctuation of the quantum well thickness leads to spatial localization of the center-of-mass wave function of the excitons and inhomogeneous broadening of the optical resonance. The inhomogeneous broadening often masks the homogeneous line widths associated with the scattering of the excitons. In addition to forming excitons, Coulombic correlations also form excitonic molecules, called biexcitons. Therefore, the coherent response of the quantum wells encompasses the intra-action and interaction of both excitons and biexcitons in the presence of inhomogeneous broadening. Transient four-wave-mixing studies combined with microscopic theories have determined that many-body interactions dominate the strong coherent response from quantum wells. Although the numerous competing interactions cannot be easily separated in either the spectral or temporal domains, they can be separated using two-dimensional Fourier transform spectroscopy.

The most common two-dimensional Fourier spectra are $S_I(\omega_\tau,T,\omega_t)$ in which the second time period is held fixed. The result is a spectrum that unfolds congested one-dimensional spectra, separates excitonic pathways, and shows which excitons are coherently coupled. This method also separates the biexciton contributions and isolates the homogeneous and inhomogeneous line widths. For semiconductor excitons, the line shape in the real part of the spectrum is sensitive to the many-body interactions, which we can suppress by exploiting polarization selection rules. In an alternative two-dimensional projection, $S_I(\tau,\omega_T,\omega_t)$, the nonradiative Raman coherent interactions are isolated. Finally, we show $S_{III}(\tau,\omega_T,\omega_t)$ spectra that isolate the two-quantum coherences associated with the biexciton. These spectra reveal previously unobserved many-body correlations.

Published on the Web 06/25/2009 www.pubs.acs.org
10.1021/ar9000636 CCC: $71.50 © 2009 American Chemical Society

Downloaded by RENMIN UNIV OF CHINA on October 2, 2009 | http://pubs.acs.org
Publication Date (Web): June 25, 2009 | doi: 10.1021/ar9000636

Introduction

Direct-gap semiconductors serve an important technological function in connecting optics and electronics based on their ability to convert light to an electronic excitation and vice versa. The use of semiconductors in this manner motivates efforts to understand many-body effects, which strongly influence the light−semiconductor interaction. At the same time, semiconductors provide a unique system for studying the fundamental physics of many-body interactions. Thus there are both applied and fundamental motivations for studying the interaction of light with semiconductors. The power of multidimensional spectroscopic techniques to disentangle a complex spectral response is providing significant advances in our understanding of how light interacts with semiconductors.

The rapid relaxation, on time scales of picoseconds to femtoseconds, of electronic excitations in semiconductors led to the use of ultrafast optics to probe carrier dynamics. However, it quickly became clear that many-body effects played an essential role in nonlinear optical measurements of semiconductors. The dominance of the many-body effects meant that they had to be understood to achieve the goal of understanding the interaction between light and semiconductors. For example, theory shows that many-body effects can shift the gain peak of a semiconductor laser.[1] In addition, optically excited semiconductors represent an ideal system for studying many-body physics.[2] An understanding was developed from one-dimensional experiments such as transient four-wave mixing (TFWM). However, many details are obscured by the presence of multiple competing phenomena. The application of optical two-dimensional Fourier transform (2DFT) spectroscopy to semiconductors has allowed these phenomena to be separated, thus improving our detailed understanding.

Linear Optics of Semiconductor Excitons

Absorption of light by a semiconductor creates an electron−hole pair by promoting an electron from the valence band to the conduction band. In a direct-gap semiconductor such as gallium arsenide (GaAs), the maximum of the valence band is aligned in momentum space with the minimum of the conduction band. This alignment is important for making direct-gap semiconductors good emitters of light, as well as good absorbers. It also allows excitons to form. Excitons are electron−hole pairs bound by their Coulomb attraction. The relative coordinate of an exciton is hydrogenic, while the center-of-mass coordinate is extended. The small masses and the high dielectric constant combine to reduce the binding energy to a few millielectronvolts; thus excitons only remain bound at low temperatures. Excitons have a strong dipole moment

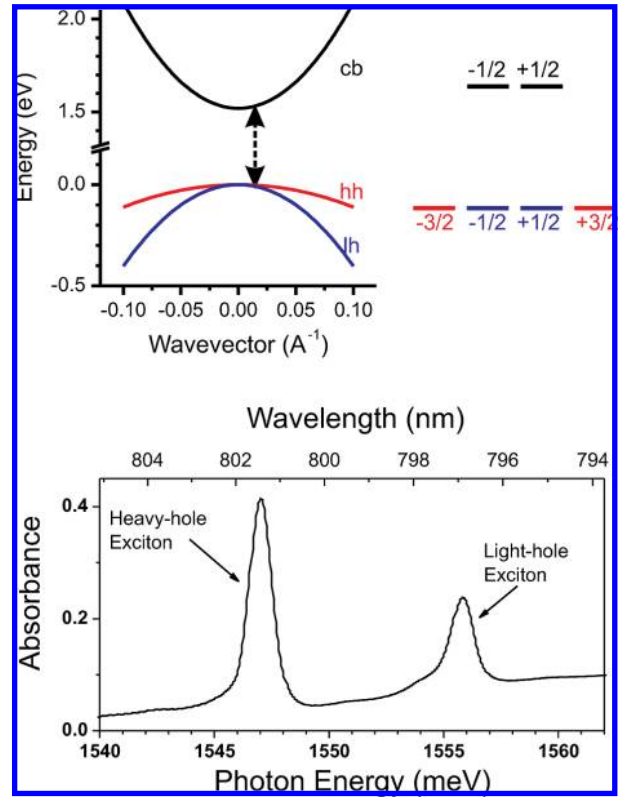

FIGURE 1. The top panel shows the band diagram of bulk GaAs (left) and magnetic substates of the three bands (right). The bottom panel shows the linear absorption spectrum of a quantum well where the degeneracy between heavy-hole and light-hole bands is lifted by quantum confinement, resulting in two exciton resonances.

because of the increased overlap between the electron and hole wave functions. At low temperature, the exciton resonances dominate the absorption and emission spectra of direct-gap semiconductors near the band edge.

The most common direct-gap semiconductor is GaAs. GaAs is common because of the established technology for epitaxial growth of high-quality heterostructures and because its band gap corresponds to near-infrared wavelengths, which are easily accessible with available lasers. A thin (∼10 nm) layer of GaAs grown between two layers of AlGaAs will display quantum confinement in the growth direction. Near the direct gap, GaAs has two valence bands, known as the heavy-hole and light-hole bands (see Figure 1, top). In bulk GaAs, the valence bands are degenerate. However, quantum confinement lifts the degeneracy. Consequently, the low-temperature linear absorption spectrum of a GaAs quantum well displays two peaks corresponding to excitons formed between conduction-band electrons and heavy or light holes (see Figure 1, bottom). In a quantum well, the heavy-hole exciton has a binding energy of approximately 10 meV.

Downloaded by RENMIN UNIV OF CHINA on October 2, 2009 | http://pubs.acs.org
Publication Date (Web): June 25, 2009 | doi: 10.1021/ar9000636

Coherent Spectroscopy of Semiconductor Excitons

Coherent spectroscopy has been used extensively to study excitons in semiconductors during the last 20 years (see ref 3 and references therein). Originally the motivation was to measure the dephasing rate of excitons. However, it quickly became clear that the signals were dominated by many-body effects. Understanding the many-body effects became the primary goal of much of the work. Structural disorder also plays a critical role in determining the optical properties of nanostructures. Coherent spectroscopy provides an important tool for separating out the effects of disorder because of its ability to "undo" the effect of inhomogeneous broadening using photon-echo techniques.

The primary coherent technique used to study excitons has been TFWM using two excitation pulses. Two pulses are incident on the sample with wavevectors $\mathbf{k}_a$ and $\mathbf{k}_b$, with delay τ between them. The coherent interaction of the pulses generates a signal in direction $\mathbf{k}_s = 2\mathbf{k}_b - \mathbf{k}_a$. For a two-level system, the signal is only emitted when $\mathbf{k}_a$ arrives before $\mathbf{k}_b$,[4] which is defined to be $\tau > 0$. TFWM can be physically described in three steps: (i) The first pulse creates a coherence. (ii) The second pulse converts the coherence to an excited-state or ground-state population depending on the relative phase between the pulses, which varies across the sample because of the angle between the pulses. Each population is spatially modulated, creating an effective grating. (iii) The second pulse scatters off of these gratings into the signal direction. The integrated TFWM signal intensity decays exponentially as a function of τ at twice the dephasing rate, γ_{ph}.

The presence of signals for "negative delay" in TFWM experiments on semiconductors was evidence for the presence of many-body interactions. These signals were phenomenologically attributed to local fields,[5] excitation-induced dephasing,[6] biexcitonic effects,[7] and excitation-induced shifts.[8] The relative strengths of these contributions could only be inferred from TFWM experiments.

Using TFWM to study disorder in quantum wells was a natural step because the signal from an inhomogeneously broadened system is a photon echo. Thus the decay of the integrated TFWM signal is $4\gamma_{ph}$ and not the inverse width of the inhomogeneous distribution. In quantum wells, the primary form of disorder is fluctuations in the well thickness, which result in fluctuations in the exciton confinement energy. While improvements in epitaxial growth techniques have improved sample quality, one monolayer of fluctuations is essentially inevitable. Localization effects of excitons in disordered quantum wells were studied because the lack of Coulomb interactions simplified the situation.[9] In quantum wells where the monolayer fluctuations were organized into large islands, the TFWM was observed to oscillate.[10] Debate arose as to whether these oscillations were due to quantum interference and thus were quantum beats or due to simple electromagnetic interference, which was dubbed "polarization interference". While the integrated TFWM signal could not make this distinction, it was shown that either temporally[11] or spectrally[12] resolving the signal could. Measurements on disordered quantum wells showed that the beats had signatures of quantum interference, which was attributed to many-body coupling between the localized excitons.[13]

The TFWM signal was observed to depend on the relative polarizations of the incident beams in surprising ways. Based on the magnetic substates shown in Figure 1, the signal polarization would depend on the incident polarizations, but other aspects would not. However, experiment showed that compared with the collinear excitation, the signal for cross-linear polarization was weaker, decayed faster,[14] and changed its temporal behavior.[15] A connection to disorder was established by comparing different samples.[16] However, it was also noticed that the excitation density mattered, suggesting that many-body effects played a role.[17] Biexcitonic effects also contributed to these observations.[7] Ultimately, numerical simulations were able to reproduce many of these effects,[18] although it was difficult to extract significant insight.

It is easier to discuss polarization effects on an excitonic basis rather than the single-particle basis presented in Figure 1. The excitonic levels for the heavy-hole exciton are shown in Figure 2. This scheme can be extended to include light-hole states.[7] An important aspect of the excitonic basis is that it naturally includes biexcitonic states. Biexcitons are bound pairs analogous to a hydrogen molecule.

The extensive work using 1D techniques, including various forms of TFWM, provided a basic understanding of many-body effects in semiconductors and how they influenced the light−matter interaction, especially for the exciton resonances. However, many aspects had to be inferred. The spectroscopic techniques were simply inadequate to address the outstanding questions.

Two-Dimensional Fourier Transform Spectroscopy

The concept of multidimensional spectroscopy originated in nuclear magnetic resonance (NMR).[19] In multidimensional spectroscopy, the nonlinear mixing of multiple electromag-

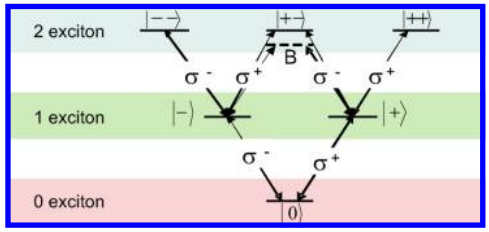

FIGURE 2. Heavy-hole states in the exciton picture. The ground state corresponds to all electrons in the valence band. For the one-exciton states, one electron has been excited to the conduction band, and it is bound to the hole it left behind to form an exciton. For the two-exciton states, a bound biexciton forms only when the electrons have opposite spin. While two excitons of the same spin do not bind to form a biexciton, they do interact. Thus the two-exciton states of same spin must be included in the level diagram. Optical transitions between exciton states are denoted by the arrows. The light must be circularly polarized to conserve spin; the helicity is denoted as σ^+ or σ^-.

netic fields in a sample produces a signal field. The signal field is recorded as a function of either the relative delays, in the case of pulsed fields, or the relative frequencies, in the case of monochromatic fields. For pulsed excitation, a spectrum is generated by a multidimensional Fourier transform, which means that the phase of the signal must be recorded and the delay scanned with steps that are equal and have subwavelength precision.

Implementing 2DFT, also known as correlation spectroscopy, with lasers was proposed in 1993.[20] The proposal was based on Raman excitation of vibrations in molecules. It was discovered that infrared excitation of molecular vibrations was experimentally preferable.[21,22] 2DFT spectroscopy was also implemented in the visible to study electronic transitions in dye molecules[23] and photosynthesis.[24]

Typically three excitation pulses are used. The incident pulses have wavevectors $\mathbf{k}_a$, $\mathbf{k}_b$, and $\mathbf{k}_c$. The interaction of the pulses in the sample produces a signal field in the direction $\mathbf{k}_s = -\mathbf{k}_a + \mathbf{k}_b + \mathbf{k}_c$. The first and second pulses have a delay τ between them, the second and third pulse have a delay T, and the emission time is t. A three-dimensional spectrum, $S_i(\tau,T,t)$, can be produced where i denotes the time ordering of the conjugated pulse, $\mathbf{k}_a$. For $S_I(\tau,T,t)$, $\mathbf{k}_a$ arrives first and dephasing due to inhomogeneous broadening is canceled because the phase accumulated during τ is reversed during t. This rephasing produces a photon echo in the presence of inhomogeneous broadening; thus it is possible to extract the homogeneous width from $S_I(\tau,T,t)$. An $S_{II}(\tau,T,t)$ spectrum has $\mathbf{k}_a$ arriving second. If $\mathbf{k}_a$ arrives last, an $S_{III}(\tau,T,t)$ spectrum is produced, which is sensitive to two-quantum coherences. The time-domain spectra are usually Fourier transformed with respect to two variables, while the third is held fixed. It is often useful to take a series of 2DFT spectra as function of the third time. The most common spectra are $S_I(\omega_\tau,T,\omega_t)$, which measures homogeneous widths, $S_I(\tau,\omega_T,\omega_t)$, which isolates Raman coherences, $S_{II}(\omega_\tau,T,\omega_t)$, which isolates coupling due to ground-state bleaching, and $S_{III}(\tau,\omega_T,\omega_t)$, which isolates two-quantum coherences.

Experimental Procedures

A schematic diagram of the experiment is shown in Figure 3. The excitation pulses propagate parallel to one another on three corners of a square. After passing through a lens, they focus to a spot size of 80 μm and overlap. The signal direction, $\mathbf{k}_s$, corresponds to the fourth corner of the square. A second lens collimates the beams and makes them parallel. The wavelength is tuned to the excitonic resonances around 800 nm. The average power per beam is 0.1 to 1 mW. Polarization optics are used to produce the desired excitation and detection conditions.

The results presented here are from a multiple quantum-well sample consisting of four periods of 10 nm thick GaAs and 10 nm thick $A1_{0.3}Ga_{0.7}As$ barriers. The sample is held at 8 K, and the incident pulses produce an excitation density between 2.5×10^9 and 2.2×10^{10} cm^{-2} per layer.

To perform a multidimensional Fourier transform on the complex signal, its phase must be measured relative to a fixed reference as a function of the delay between the excitation pulses. The delay must be stable and stepped with subwavelength accuracy. To decompose the complex spectrum into real and imaginary parts, which can be related to the complex third-order susceptibility, experimental phase shifts must be removed by adjusting the "global" phase of the as-measured spectra. The spectra actually correspond to real and imaginary parts of the signal field. The phase shift between polarization in the sample and radiated field needs to be considered to determine the susceptibility.

Phase-Locked Excitation. The phase-locked excitation pulses are produced by an actively stabilized apparatus.[25] The error signal for the servo loop is generated from the interference of an auxiliary HeNe laser beam that copropagates with the femtosecond pulses. Four phase-locked pulses are produced by using nested and folded interferometers. The HeNe laser is retroreflected by a dichroic beam splitter such that it double passes the interferometers. Locking the interferometers using the servo loop provides a fixed delay between the pulses. To change the delay, the servo loops are disabled, and the delay is stepped while the error signals are monitored. When the delay has been changed by the desired amount and the error signal is close

Downloaded by RENMIN UNIV OF CHINA on October 2, 2009 | http://pubs.acs.org
Publication Date (Web): June 25, 2009 | doi: 10.1021/ar9000636

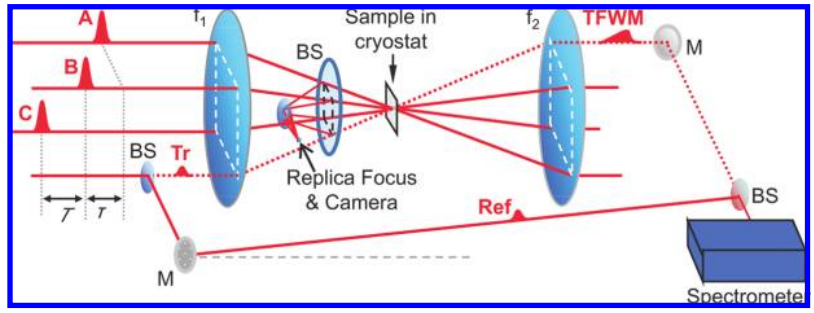

FIGURE 3. Experimental apparatus.

to a zero crossing, the servo loops are re-enabled, which drives the error signal to zero. Three of the beams are used as excitation beams. The fourth is used as a "tracer" beam.

Signal Field Measurement. The electric field of the signal is measured using spectral interferometry.[26] Spectral interferometry allows the phase and amplitude of an unknown signal pulse to be extracted by comparing it to a reference pulse. In principle, the tracer pulse could serve as the reference for spectral interferometry because it copropagates with the signal. However, excitation-induced effects in the sample lead to artifacts if the reference pulse goes through the sample. Thus, we derive a reference pulse from the tracer and route it around the sample and cryostat.

Since the overall (constant) signal phase, not just its spectral variation, is needed, the reference beam must have a stable phase throughout the acquisition of a 2DFT spectrum. Unfortunately, the stability of the reference is compromised by routing it around the sample. Thus an additional feedback loop is needed.

Global Phase. A 2DFT spectrum can be decomposed into real and imaginary parts related to the third-order complex susceptibility. However the decomposition requires that the overall, or "global", phase be correctly set. The real and imaginary parts are useful because they reflect the underlying physical processes. Additionally, the spectral resolution can be enhanced by suppressing dispersive wings. However, the as-measured 2DFT spectrum has phase offsets that must be corrected. In our apparatus, these phase offsets arise from the relative phase of the excitation pulses at zero delay, from the reference phase relative to the third pulse, and from phase shifts between the signal and reference pulses. Previously, these phase offsets were determined by comparing the complex signal spectrum at zero delay to an auxiliary transient absorption spectrum.[25] However, this technique proved to be problematic in semiconductors. Furthermore, the appropriate auxiliary experiment is difficult for some 2DFT spectra such as cross-polarized excitation or two-quantum coherences.

Recently, we developed an alternative method, based on the spatial interference pattern at the sample position, for determining the global phase.[27] A similar method was independently developed for use in infrared 2DFT experiments.[28] The spatial interference pattern between the excitation beams, including the tracer beam, depends on the relative phases in the same way as the 2DFT spectrum. By recording the pattern, it is possible to determine the phase differences. The phase shift between the reference and tracer, as well as propagation-induced phases shifts, are determined by recording appropriate spectral interferograms.

Co-polarized S_I

A typical $S_I(\omega_\tau,T,\omega_t)$ of the heavy- and light-hole excitons is shown in Figure 4. This figure shows the real spectrum. The laser spectrum is tuned to be centered between the two excitonic resonances. The excitation pulses are collinearly polarized. The 2DFT spectrum displays two diagonal peaks for the heavy- and light-hole excitons. The heavy-hole peak line shape is "dispersive" in that it is negative above the diagonal and positive below it. For a simple few-level system, the real $S_I(\omega_\tau,T,\omega_t)$ should display an "absorptive" line shape, that is, one that is purely positive. The dispersive line shape occurs because the excitonic response is dominated by many-body effects.[29,30] The cross peaks between the excitons are expected for collinear polarization. For this laser tuning, their strength lies between those of the diagonal peaks. If the laser is tuned to be centered on the light hole, the lower left cross peak (labeled "c" in the figure) becomes the strongest feature. For a few-level system, a cross peak can never be the strongest feature. Many-body interactions between the two excitons can result in a dominant cross peak.[31] Similarly, the many-body interaction between the continuum and heavy-hole exciton results in a vertical feature, whereas a diagonal feature is expected without many-body contributions.[31]

Downloaded by RENMIN UNIV OF CHINA on October 2, 2009 | http://pubs.acs.org
Publication Date (Web): June 25, 2009 | doi: 10.1021/ar9000636

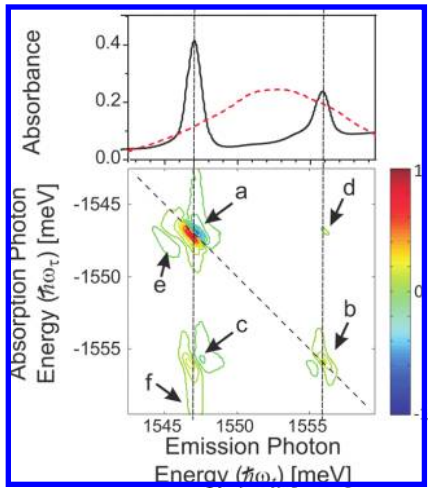

FIGURE 4. The lower panel shows the real 2DFT spectrum, $S_I(\omega_\tau,T,\omega_t)$, of the heavy- and light-hole resonances for collinearly polarized excitation. The upper panel shows the linear absorption spectrum (black line) and the spectrum of the excitation pulses (red line). The photon energies of the exciton resonances are marked by dashed lines. The 2DFT spectrum shows diagonal peaks due the heavy- and light-hole excitons, labeled "a" and "b", respectively. Cross-peaks between the excitons are marked as "c" and "d". The feature "e" is the biexciton formed from heavy-hole excitons. The continuum contribution is the vertical feature "f".

The elongation of the heavy-hole peak along the diagonal is due to inhomogeneous broadening. In a semiconductor quantum well, inhomogeneous broadening occurs because of unavoidable fluctuation in the well width. Since the quantum confinement energy is inversely proportional to the width, width fluctuations result in static fluctuations of the resonance energy. Both the homogeneous and inhomogeneous widths can be extracted from the 2DFT spectrum. The extraction is aided by comparing $S_I(\omega_\tau,T,\omega_t)$ to $S_{II}(\omega_\tau,T,\omega_t)$.[32] Disorder can localize the electronic states, reducing the strength of many-body interactions.

One of the intriguing features is the peak "e", which is slightly negative due to the formation of biexcitons. For a few-level system, the positive diagonal peaks correspond to a reduction in the absorption. The generation of biexcitons results in an increase in the absorption and thus should have the opposite sign. Based on the level diagram in Figure 2, the strength of the biexciton peak should be half that of the exciton peak. It is much weaker than that because many-body effects enhance the exciton peak but not the biexciton peak.

Cross-Polarized S_I

The $S_I(\omega_\tau,T,\omega_t)$ spectrum is shown in Figure 5 for the same conditions as Figure 4, except that the first pulse is cross-polarized. The component of the signal that is co-polarized with the first pulse is detected. The overall signal is much weaker. More dramatic changes are the line shape of the

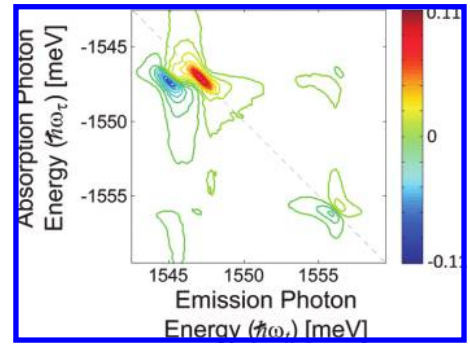

FIGURE 5. The 2DFT spectrum, $S_I(\omega_\tau,T,\omega_t)$, of the heavy- and light-hole resonances of a GaAs quantum well with cross-linearly polarized excitation. The numerical values on the color bar are relative to Figure 4.

heavy-hole exciton diagonal peak and its strength relative to the biexciton peak. The line shape is now absorptive, whereas for co-polarized excitation, it was dispersive.

These changes occur because cross-polarized excitation suppresses many-body contributions, which can be explained in terms of the physical picture for the TFWM signal given above. For cross-polarized excitation, the population grating induced in the $|+\rangle$ exciton is π out of phase with that for the $|-\rangle$ exciton. Consequently, there is no net population grating. Since the many-body interactions are thought to be spin independent,[6] they are spatially uniform and thus do not give a signal. While this understanding had been inferred, the change in the line shape from dispersive in Figure 4 to absorptive in Figure 5 confirms this interpretation.

The biexciton peaks in Figures 4 and 5 demonstrate a powerful feature of 2DFT spectroscopy. Biexcitonic features have been observed in photoluminescence and TFWM experiments. In photoluminescence, biexcitons appear as a low-energy shoulder on the exciton line that grows quadratically with excitation intensity. In GaAs quantum wells, the biexciton peak is never resolved from the exciton peak. In the 2DFT spectrum, both peaks show diagonal elongation, resulting in resolved peaks. The diagonal broadening of the biexciton peak shows that it is inhomogeneously broadened by well-width fluctuations. Moreover, it shows that the two excitons making up the biexciton experience correlated inhomogeneity. Thus they exist on the same localization site.

The isolation of the biexciton allows its properties to be studied. For example, the "ridge" of the biexciton line is not exactly diagonal, suggesting that the biexciton binding energy varies with the strength of the localization. The homogeneous line width of the biexciton can be extracted

Downloaded by RENMIN UNIV OF CHINA on October 2, 2009 | http://pubs.acs.org
Publication Date (Web): June 25, 2009 | doi: 10.1021/ar9000636

as a function of position within the inhomogeneous distribution, which was not possible using 1D spectroscopies.

Nonradiative Coherences

An advantage of 2DFT spectroscopy is its ability to isolate nonradiative coherences, that is, coherences between states that are not coupled by a dipole matrix element. While these transitions do not interact directly with light, they do result in oscillations in some 1D experiments.[33−35] However, in 1D experiments, they generally cannot be isolated from other contributions, which means that care is needed in interpreting the results.[36]

In 2DFT experiments, a nonradiative coherence can be created during one of the time periods, typically the second period, and then converted to a radiative coherence. The phase evolution while the system is in the nonradiative coherence sets the initial phase of the radiative coherence. Thus by recording the signal from the radiative coherence and taking a Fourier transform with respect to the time delay corresponding to the nonradiative coherence, it can be isolated.

In GaAs quantum wells, there are two examples of nonradiative coherences. The first is a coherence established between the heavy-hole and light-hole exciton states.[34−36] Since these states are similar in energy, these coherences are often known as "Raman" coherences. The other example is a coherence established between the ground state and a doubly excited state such as a biexciton.[33,37] These coherences are known as "two-quantum" coherences.

"Raman" Coherences in S_I. The Raman coherence between the heavy- and light-hole excitons contributes to the spectra in Figures 4 and 5. Specifically, they appear in the off-diagonal peaks labeled "c" and "d" in Figure 4. These peaks also contain contributions due to coupling between the two excitons via bleaching of the ground state. By a scan of the second delay, it is possible to produce a different spectrum, $S_I(\tau,\omega_T,\omega_t)$, that separates these contributions and produces a peak due only to the Raman coherences.[38]

Figure 6 shows an experimental $S_I(\tau,\omega_T,\omega_t)$ spectrum. The peaks at $\hbar\omega_T = 0$ contain all the contributions from pathways that correspond to excited-state emission or ground-state bleaching. Theoretical results agree well with these experimental results.[39]

The widths of the Raman peaks give information about scattering processes that affect the relative energy of the two-exciton states. Comparison of the width of the peaks in the corresponding $S_I(\omega_\tau,T,\omega_t)$ spectrum and their dependences on parameters such as carrier density and temperature yield greater insight into the nature of the scattering processes. For example, it is possible to determine whether the fluctuations in the energy levels that cause dephasing are correlated or anticorrelated.[35]

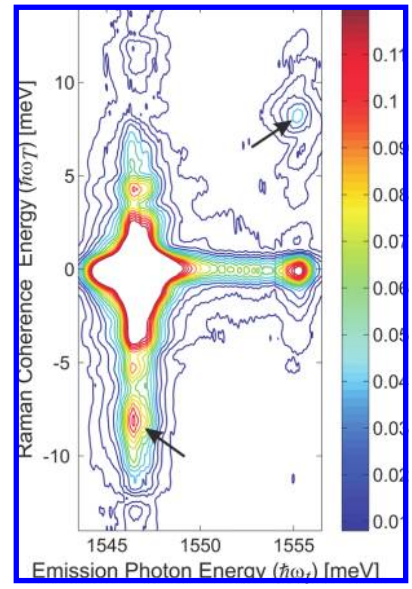

FIGURE 6. The magnitude 2DFT spectrum, $S_I(\tau,\omega_T,\omega_t)$, of the heavy- and light-hole resonances of a GaAs quantum well for collinearly polarized excitation. The arrows point to spectral peaks due to Raman coherence between the excitons. The intensity scale has been set so that the central peaks ($\omega_T = 0$) saturate.

Two-Quantum Coherences in S_{III}. A two-quantum coherence occurs between the ground state and a doubly excited state. In our case, a two-quantum coherence between the ground state and a biexciton is expected. However, two-quantum coherences involving doubly excited many-body states also occur.[37,40,41] Two-dimensional spectroscopy allows these contributions to be distinguished, which was not possible in previous 1D experiments.[33]

To observe a two-quantum coherence, the conjugated pulse must arrive third because the first two pulses both increase the excitation level of the system to reach the doubly excited state. The third pulse either de-excites the system to establish a radiative coherence between the ground state and a singly excited state or acts on the opposite side of the density matrix to establish a radiative coherence between singly and doubly excited states. Since the two-quantum coherence exists during the second time period, the Fourier transform is taken with respect to T. Thus a two-quantum coherence appears in a $S_{III}(\tau,\omega_T,\omega_t)$ spectrum at $\omega_T \approx 2\omega_t$ because the two-quantum coherence evolves at a frequency corresponding to the energy difference between the ground state and the doubly excited state.

The $S_{III}(\tau,\omega_T,\omega_t)$ spectrum of the heavy-hole resonance is shown in Figure 7 for circularly polarized excitation. In the left

Downloaded by RENMIN UNIV OF CHINA on October 2, 2009 | http://pubs.acs.org
Publication Date (Web): June 25, 2009 | doi: 10.1021/ar9000636

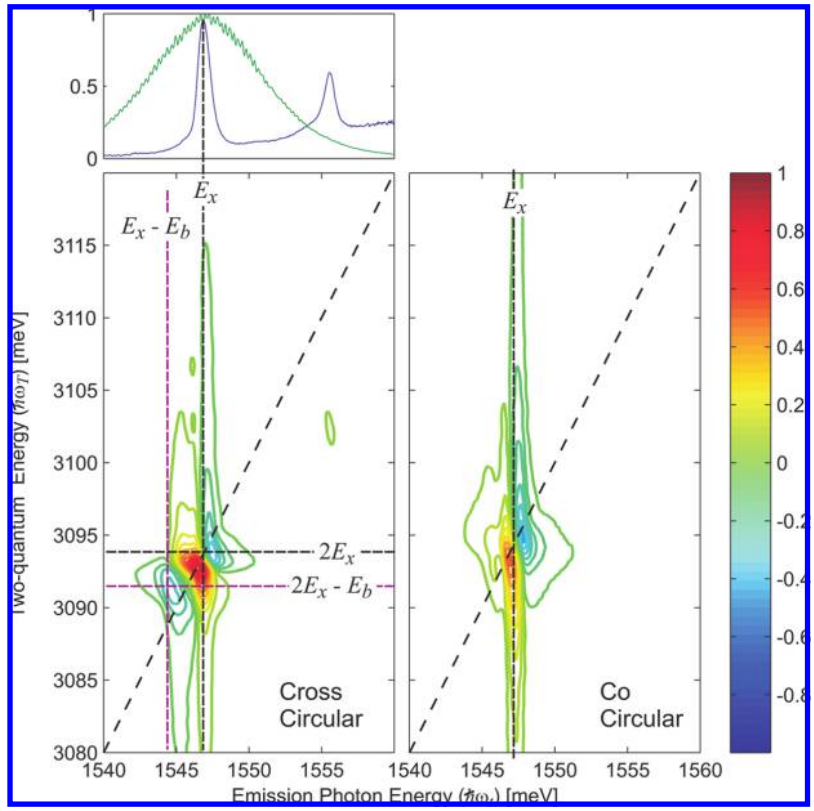

FIGURE 7. The 2DFT spectrum, $S_{III}(\tau,\omega_T,\omega_t)$, of the heavy-hole resonance of a GaAs quantum well for cross-circular (left) and cocircular (right) excitation.

Downloaded by RENMIN UNIV OF CHINA on October 2, 2009 | http://pubs.acs.org
Publication Date (Web): June 25, 2009 | doi: 10.1021/ar9000636

panel, the first pulse has opposite helicity compared with the second and third pulses. In this case, bound-biexciton states can be accessed, as per Figure 2. Based on the level scheme, two-quantum resonances would be expected at coordinates ($\hbar\omega_T = 2E_x - E_b$, $\hbar\omega_t = E_x - E_b$) and ($2E_x - E_b$, E_x) where E_x is the photon energy of the exciton resonance and E_b is the biexciton binding energy. These peaks have opposite signs with the first being negative, as expected from perturbation theory. However, the strongest feature in the spectrum occurs at ($2E_x$,E_x) and has a dispersive line shape. This peak is attributed to two-quantum coherence involving a many-body state, rather than a biexciton. To test the assignment, a spectrum was taken with cocircularly polarized pulses (right panel). As expected, the features ascribed to the biexciton are suppressed, while the dispersive many-body peak remains, although it is slightly shifted to higher energy.

2DFT spectra showing that two-quantum coherences occur between the ground state and a many-body state demonstrate the power of the technique. Previous measurements did not provide evidence for the existence of two-quantum coherences involving many-body states.

Summary and Outlook

The application of two-dimensional Fourier transform spectroscopy to semiconductors demonstrates the power of the technique to separate and isolate the many contributions to the coherent optical response. The results show that many-body contributions dominate the response in most situations, although they can be suppressed using polarization. Contributions from biexcitonic states can be isolated, even in the presence of inhomogeneous broadening due to disorder. The ability to isolate them will aid in studies of their energetics and dynamics. Isolation of nonradiative Raman and two-quantum coherences also facilitates understanding them. The presence of two-quantum coherences involving many-body states, rather than biexcitons, further motivates future work using this technique.

We acknowledge discussions with Peter Thomas and Irina Kuznetsova from the University of Marburg, Germany; with Torsten Meier from the University of Paderborn, Germany; and with Shaul Mukamel and Lijun Yang from the University of California, Irvine. We acknowledge Richard Mirin of the National Institute of Standards and Technology in Boulder for providing the epitaxially grown samples. This work was funded by the Chemical Sciences, Geosciences, and Biosciences Division of the Office of Basic Energy Science, U.S. Department of Energy, and the National Science Foundation.

Downloaded by RENMIN UNIV OF CHINA on October 2, 2009 | http://pubs.acs.org
Publication Date (Web): June 25, 2009 | doi: 10.1021/ar9000636

BIOGRAPHICAL INFORMATION

Steven T. Cundiff is a Fellow of JILA, a joint institute between the National Institute of Standards and Technology and the University of Colorado at Boulder. In 1992, he received his Ph.D. in Applied Physics from the University of Michigan. He spent two years at the University of Marburg, Germany, as a von Humboldt Post-doctoral Fellow. After that he was at Bell Laboratories, Holmdel, until joining JILA in 1997. He is a Fellow of the American Physical Society and the Optical Society of America.

Tianhao Zhang received his Ph.D. degree in Physics from the University of Colorado in 2008. He is currently a postdoctoral research associate in the College of Nanoscale Science and Engineering, State University of New York at Albany.

Alan D. Bristow received his Ph.D. from the University of Sheffield in the U.K. (2003). From 2003to 2006, he was a Postdoctoral Fellow at the University of Toronto in Canada, and he is now a Research Associate at JILA (University of Colorado and National Institute of Standards and Technology). His research interests are in light−matter interactions of condensed-matter nanostructures and nanophotonic materials.

Denis Karaiskaj received his Diplom in Physics from the University of Marburg, Germany, and his Ph.D. in Physics from Simon Fraser University, Canada. He was a postdoctoral scientist at the University of California, Irvine, and then a Post-doctoral Fellow and Research Scientist at the National Renewable Energy Laboratory in Golden, Colorado. Currently, he is a Research Associate at JILA.

Xingcan Dai earned his Ph.D. in Physics in 2006 from the University of California, Berkeley. He is currently a Research Associate at JILA. His research interests lie in ultrafast spectroscopy of dense atomic vapors and semiconductors.

FOOTNOTES

*To whom correspondence should be addressed. E-mail: adb@jila.colorado.edu, Dr. Bristow

§Current address: College of Nanoscale Science and Engineering, State University of New York at Albany, 255 Fuller Rd., Albany, NY 12203.

REFERENCES

1 Chow, W.; Koch, S.; Sargent, M. *Semiconductor-Laser Physics*; Springer-Verlag: Berlin, 1994.

2 Chemla, D. S.; Shah, J. Many-body and correlation effects in semiconductors. *Nature* **2001**, *411*, 549–557.

3 Cundiff, S. T. Coherent spectroscopy of semiconductors. *Opt. Express* **2008**, *16*, 4639–4664.

4 Yajima, T.; Taira, Y. Spatial optical parametric coupling of picosecond light-pulses and transverse relaxation effect in resonant media. *J. Phys. Soc. Jpn.* **1979**, *47*, 1620–1626.

5 Leo, K.; Wegener, M.; Shah, J.; Chemla, D. S.; Göbel, E. O.; Damen, T. C.; Schmitt-Rink, S.; Schäfer, W. Effects of coherent polarization interactions on time-resolved degenerate 4-wave-mixing. *Phys. Rev. Lett.* **1990**, *65*, 1340–1343.

6 Wang, H. L.; Ferrio, K.; Steel, D. G.; Hu, Y. Z.; Binder, R.; Koch, S. W. Transient nonlinear-optical response from excitation induced dephasing in GaAs. *Phys. Rev. Lett.* **1993**, *71*, 1261–1264.

7 Bott, K.; Heller, O.; Bennhardt, D.; Cundiff, S. T.; Thomas, P.; Mayer, E. J.; Smith, G. O.; Eccleston, R.; Kuhl, J.; Ploog, K. Influence of exciton-exciton interactions on the coherent optical-response in GaAs quantum-wells. *Phys. Rev. B* **1993**, *48*, 17418–17426.

8 Shacklette, J. M.; Cundiff, S. T. Role of excitation-induced shift in the coherent optical response of semiconductors. *Phys. Rev. B* **2002**, *66*, 045309.

9 Hegarty, J.; Sturge, M. D. Studies of exciton localization in quantum-well structures by nonlinear-optical techniques. *J. Opt. Soc. Am. B* **1985**, *2*, 1143–1154.

10 Göbel, E. O.; Leo, K.; Damen, T. C.; Shah, J.; Schmitt-Rink, S.; Schäfer, W.; Muller, J. F.; Köhler, K. Quantum beats of excitons in quantum-wells. *Phys. Rev. Lett.* **1990**, *64*, 1801–1804.

11 Koch, M.; Feldmann, J.; von Plessen, G.; Göbel, E. O.; Thomas, P.; Kohler, K. Quantum beats versus polarization interference - an experimental distinction. *Phys. Rev. Lett.* **1992**, *69*, 3631–3634.

12 Lyssenko, V. G.; Erland, J.; Balslev, I.; Pantke, K. H.; Razbirin, B. S.; Hvam, J. M. Nature of nonlinear 4-wave-mixing beats in semiconductors. *Phys. Rev. B* **1993**, *48*, 5720–5723.

13 Jahnke, F.; Koch, M.; Meier, T.; Feldmann, J.; Schäfer, W.; Nickel, H.; Thomas, P.; Koch, S. W.; Göbel, E. O. Simultaneous influence of disorder and Coulomb interaction on photon-echoes in semiconductors. *Phys. Rev. B* **1994**, *50*, 8114–8117.

14 Yaffe, H. H.; Prior, Y.; Harbison, J. P.; Florez, L. T. Polarization dependence and selection rules of transient four-wave mixing in GaAs quantum-well excitons. *J. Opt. Soc. Am. B* **1993**, *10*, 578–583.

15 Cundiff, S. T.; Wang, H.; Steel, D. G. Polarization-dependent picosecond excitonic nonlinearities and the complexities of disorder. *Phys. Rev. B* **1992**, *46*, 7248–7251.

16 Bennhardt, D.; Thomas, P.; Eccleston, R.; Mayer, E. J.; Kuhl, J. Polarization dependence of four-wave-mixing signals in quantum wells. *Phys. Rev. B* **1993**, *47*, 13485–13490.

17 Eccleston, R.; Kuhl, J.; Bennhardt, D.; Thomas, P. Intensity dependent four-wave-mixing polarization rules in quantum wells. *Solid State Commun.* **1993**, *86*, 93–97.

18 Weiser, S.; Meier, T.; Mobius, J.; Euteneuer, A.; Mayer, E. J.; Stolz, W.; Hofmann, M.; Ruhle, W. W.; Thomas, P.; Koch, S. W. Disorder-induced dephasing in semiconductors. *Phys. Rev. B* **2000**, *61*, 13088–13098.

19 Ernst, R.; Bodenhausen, G.; Wokaun, A. *Principles of Nuclear Magnetic Resonance in One and Two Dimensions*; Oxford Science Publications: Oxford, U.K., 1987.

20 Tanimura, Y.; Mukamel, S. 2-Dimensional femtosecond vibrational spectroscopy of liquids. *J. Chem. Phys.* **1993**, *99*, 9496–9511.

21 Asplund, M. C.; Zanni, M. T.; Hochstrasser, R. M. Two-dimensional infrared spectroscopy of peptides by phase-controlled femtosecond vibrational photon echoes. *Proc. Natl. Acad. Sci. U.S.A.* **2000**, *97*, 8219–8224.

22 Golonzka, O.; Khalil, M.; Demirdöven, N.; Tokmakoff, A. Vibrational anharmonicities revealed by coherent two-dimensional infrared spectroscopy. *Phys. Rev. Lett.* **2001**, *86*, 2154–2157.

23 Hybl, J.; Ferro, A.; Jonas, D. Two-dimensional Fourier transform electronic spectroscopy. *J. Chem. Phys.* **2001**, *115*, 6606–6622.

24 Brixner, T.; Stenger, J.; Vaswani, H.; Cho, M.; Blankenship, R.; Fleming, G. Two-dimensional spectroscopy of electronic couplings in photosynthesis. *Nature* **2005**, *434*, 625–628.

25 Zhang, T. H.; Borca, C. N.; Li, X. Q.; Cundiff, S. T. Optical two-dimensional Fourier transform spectroscopy with active interferometric stabilization. *Opt. Express* **2005**, *13*, 7432–7441.

26 Lepetit, L.; Cheriaux, G.; Joffre, M. Linear techniques of phase measurement by femtosecond spectral interferometry for applications in spectroscopy. *J. Opt. Soc. Am. B* **1995**, *12*, 2467.

27 Bristow, A. D.; Karaiskaj, D.; Dai, X.; Cundiff, S. T. All-optical retrieval of the global phase for two-dimensional Fourier-transform spectroscopy. *Opt. Express* **2008**, *16*, 18017–18027.

28 Backus, E. H. G.; Garrett-Roe, S.; Hamm, P. Phasing problem of heterodyne-detected twodimensional infrared spectroscopy. *Opt. Lett.* **2008**, *33*, 2665–2667.

29 Li, X. Q.; Zhang, T. H.; Borca, C. N.; Cundiff, S. T. Many-body interactions in semiconductors probed by optical two-dimensional Fourier transform spectroscopy. *Phys. Rev. Lett.* **2006**, *96*, 057406.

30 Zhang, T.; Kuznetsova, I.; Meier, T.; Li, X.; Mirin, R.; Thomas, P.; Cundiff, S. Polarizationdependent optical 2D Fourier transform spectroscopy of semiconductors. *Proc. Natl. Acad. Sci. U.S.A.* **2007**, *104*, 14227–14232.

31 Borca, C. N.; Zhang, T. H.; Li, X. Q.; Cundiff, S. T. Optical two-dimensional Fourier transform spectroscopy of semiconductors. *Chem. Phys. Lett.* **2005**, *416*, 311–315.

32 Kuznetsova, I.; Meier, T.; Cundiff, S. T.; Thomas, P. Determination of homogeneous and inhomogeneous broadening in semiconductor nanostructures by two-dimensional Fouriertransform optical spectroscopy. *Phys. Rev. B* **2007**, *76*, 153301.

33 Ferrio, K. B.; Steel, D. G. Observation of the ultrafast two-photon coherent biexciton oscillation in a GaAs/AlxGa1-xAs multiple quantum well. *Phys. Rev. B* **1996**, *54*, R5231–R5234.

34 Ferrio, K. B.; Steel, D. G. Raman quantum beats of interacting excitons. *Phys. Rev. Lett.* **1998**, *80*, 786–789.

35 Spivey, A. G. V.; Borca, C. N.; Cundiff, S. T. Correlation coefficient for dephasing of lighthole excitons and heavy-hole excitons in GaAs quantum wells. *Solid State Commun.* **2008**, *145*, 303–307.

36 Hawkins, S. A.; Gansen, E. J.; Stevens, M. J.; Smirl, A. L.; Rumyantsev, I.; Takayama, R.; Kwong, N. H.; Binder, R.; Steel, D. G. Differential measurements of

Raman coherence and two-exciton correlations in quantum wells. *Phys. Rev. B* **2003**, *68*, 035313.

37 Stone, K. W.; Gundogdu, K.; Turner, D. B.; Li, X.; Cundiff, S. T.; Nelson, K. A. Two-quantum 2D FT electronic spectroscopy of biexcitons in GaAs quantum wells. *Science* **2009**, in press.

38 Yang, L. J.; Schweigert, I. V.; Cundiff, S. T.; Mukamel, S. Two-dimensional optical spectroscopy of excitons in semiconductor quantum wells: Liouville-space pathway analysis. *Phys. Rev. B* **2007**, *75*, 125302.

39 Yang, L.; Zhang, T.; Bristow, A. D.; Cundiff, S. T.; Mukamel, S. Isolating excitonic Raman coherence in semiconductors using two-dimensional correlation spectroscopy. *J. Chem. Phys.* **2008**, *129*, 234711.

40 Yang, L.; Mukamel, S. Two-dimensional correlation spectroscopy of two-exciton resonances in semiconductor quantum wells. *Phys. Rev. Lett.* **2008**, *100*, 057402.

41 Stone, K. W.; Turner, D. B.; Gundogdu, K.; Cundiff, S. T.; Nelson, K. A. Exciton−exciton correlations revealed by two-quantum two-dimensional Fourier Transform Optical Spectroscopy. *Acc. Chem. Res.* **2009**, submitted for publication.

42 Bristow, A. D.; Karaiskaj, D.; Dai, X.; Mirin, R. P.; Cundiff, S. T. Polarization dependence of semiconductor exciton and biexciton contributions to phase-resolved optical two-dimensional Fourier-transform spectra. *Phys. Rev. B* **2009**, *79*, 161305(R).

Downloaded by RENMIN UNIV OF CHINA on October 2, 2009 | http://pubs.acs.org
Publication Date (Web): June 25, 2009 | doi: 10.1021/ar9000636